

# RIKEN RI-BEAM FACTORY PROJECT

Y. Yano and A. Goto, RIKEN Wako, Saitama 351-01, Japan and  
T. Katayama, Center for Nuclear Study, School of Science,  
University of Tokyo Tanashi, Tokyo 188, Japan

## Abstract

The RIKEN Accelerator Research Facility (RARF) has proposed the "RI-Beam Factory" project. In 1997 fiscal year, the construction budget for the first phase of this project has been formally approved. The factory is aimed at providing the world's most intense RI (radioisotope) beams at energies of several hundreds MeV/nucleon over the whole range of atomic masses. RI beams will be generated by the projectile fragmentation. For the efficient generation a cascade of a K930-MeV ring cyclotron and a K2500-MeV super-conducting ring cyclotron will boost the energy of heavy-ion beams from the existing ring cyclotron up to 400 MeV/nucleon for light ions and more than 100 MeV/nucleon for very heavy ions. Moreover, this factory includes a next generation of the multi-use experimental storage rings (MUSES) consisting of an accumulator-cooler ring, a booster synchrotron ring and double storage rings. The MUSES will enable us to conduct various types of unique colliding experiments.

## 1 INTRODUCTION

The RARF (RIKEN Accelerator Research Facility) has a heavy-ion accelerator complex consisting of a K540-MeV ring cyclotron (RRC) as a main accelerator and two different types of injectors: a frequency-variable Wideröe linac (RILAC) and a K70-MeV AVF cyclotron (AVF). The facility provides heavy-ion (HI) beams over the whole atomic mass range and in a wide energy range from 0.6 MeV/nucleon to 135 MeV/nucleon. One of the

remarkable features of this facility is capability of supplying light-atomic-mass RI (radioisotope) beams with the world-highest level of intensity which are produced by means of the projectile-fragment separator, RIPS [1].

In order to further promote experimental programs utilizing RI beams, the RARF undertakes the construction of "RI Beam Factory". The bird's eye view of its layout is illustrated in Fig. 1. The factory is aimed at providing RI beams covering over the whole atomic-mass range with very high intensity in a wide energy range up to several hundreds MeV/nucleon.

## 2 A CASCADE OF CYCLOTRONS FOR HIGH-INTENSITY RI BEAM PRODUCTION

The factory utilizes the "projectile fragmentation" to generate RI beams of intermediate energies. To enable the efficient generation of such RI beams covering the whole atomic masses, are needed high-intensity primary heavy-ions, up to uranium ions, with the energies exceeding 100 MeV/nucleon. In order to realize those beams, we will construct a cascade of an intermediate-stage ring cyclotron (IRC) with K=930 MeV and a superconducting ring cyclotron (SRC) with K=2500 MeV as an energy booster of the existing RRC. In addition, we will upgrade the RILAC which serves as the initial-stage accelerator by introducing a new pre-injector and a charge-state multiplier (CSM). This accelerator complex, which is schematically illustrated in Fig. 2, will possess such performance that a 100 MeV/nucleon uranium beam with the intensity over 1 pμA is obtainable.

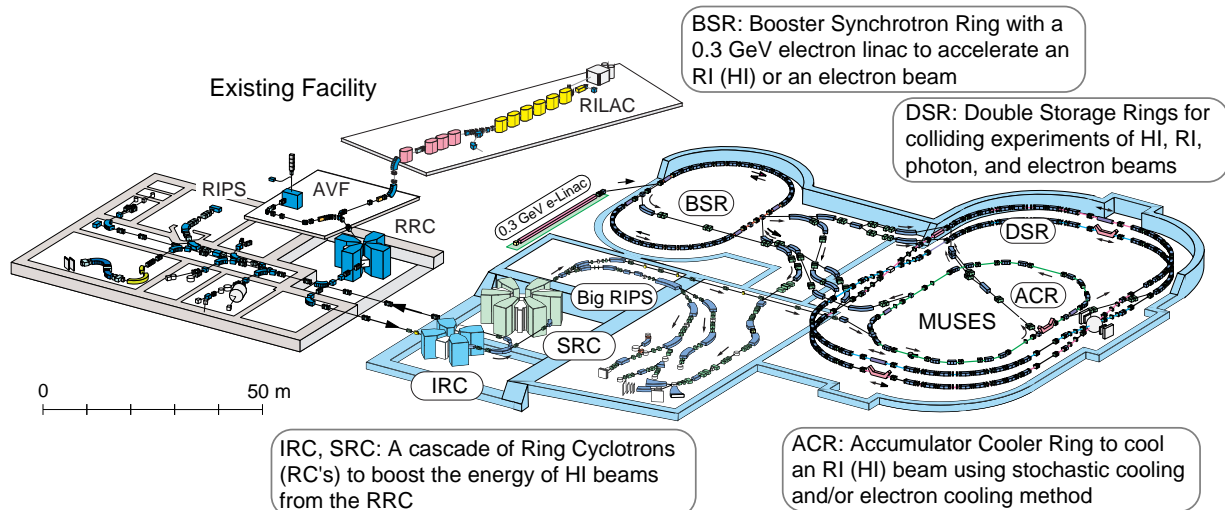


Fig. 1 Bird's eye view of "RI-Beam Factory" layout.

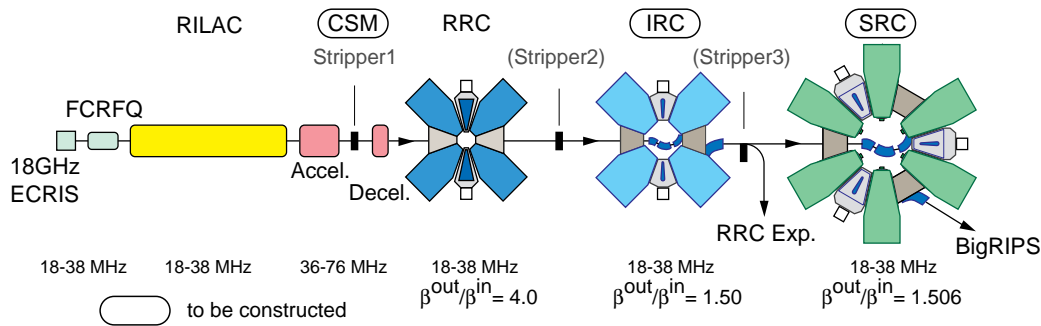


Fig. 2 Conceptual diagram of heavy-ion accelerator complex for RI-beam production.

### 2.1 Pre-injector for RILAC

The RILAC is stably operational in the acceleration radio-frequency range between 18 MHz and 38 MHz. In order to upgrade the RILAC performance in the beam intensity by one or two orders of magnitude, its new pre-injector system consisting of a frequency-tunable folded-coaxial RFQ linac (FC-RFQ) equipped with an 18-GHz ECR ion source (ECRIS-18) has been developed. In the recent acceleration tests, the FC-RFQ has successfully covered HI beams in the energy-mass region required, and the beam transmission efficiency of about 90 % at the maximum was obtained [2]. In addition, high-intensity highly-charged ion beams have been produced by the ECRIS-18 [3].

### 2.2 CSM

The CSM consists of an accelerator, a charge stripper and a decelerator. Its functions are to produce higher charge state of ion beams by further increasing the stripping energy and to reduce their magnetic rigidity by decelerating them to the initial energy. With this device the magnetic rigidity of the RILAC beam with a most-probable charge state can be reduced to the acceptable value of the RRC even when the injection velocity into the RRC is increased as shown in Fig. 3. The accelerator and decelerator are of a type of frequency-tunable IH linac whose operational radio-frequencies are twice as that of the RILAC to double an acceleration gradient. Transmission efficiency through the CSM depends only on charge state distribution behind the charge stripper foil.

### 2.3 IRC-SRC

The maximum beam energy of the SRC is set to be 400 MeV/nucleon for light ions which is achieved at 38 MHz, the maximum radio-frequency in the RILAC. Based on the characteristics of the existing machines, this means that the velocity of the RRC's output beam has to be amplified by a factor of 2.26 by combination of the IRC and the SRC. Harmonic numbers of the IRC and the SRC are chosen to be 7 and 6, respectively, while that of the RRC is 9, considering the maximum magnetic field strength and the central space to place the injection elements. The mean injection radius of the IRC is taken to be 7/9 times the mean extraction radius of the RRC,

and the velocity gain factor of the IRC to be 1.50 (accordingly that of SRC is to be 1.506). On the above conditions, the mean injection and extraction radii of the IRC are 2.77 m and 4.15 m, respectively, and those of the SRC are 3.56 m and 5.36 m, respectively. The sector angles are taken to be 51° for the IRC and 25° for the SRC, based on the beam dynamics study [4]. The radio-frequency of the IRC and the SRC ranges from 18 MHz to 38 MHz which are the same as that of the RILAC and the RRC. The maximum magnetic field strength in the sector magnets is to be 1.9 T for the IRC and 4.3 T for the SRC. This IRC-SRC system boosts the energy of uranium ions from the RRC up to more than 100 MeV/nucleon.

Geometries and characteristics of the IRC and the SRC thus designed are shown in Fig. 4 along with those of the RRC. The structure and size of the IRC are similar to those of the RRC, and the rf resonators of the IRC and

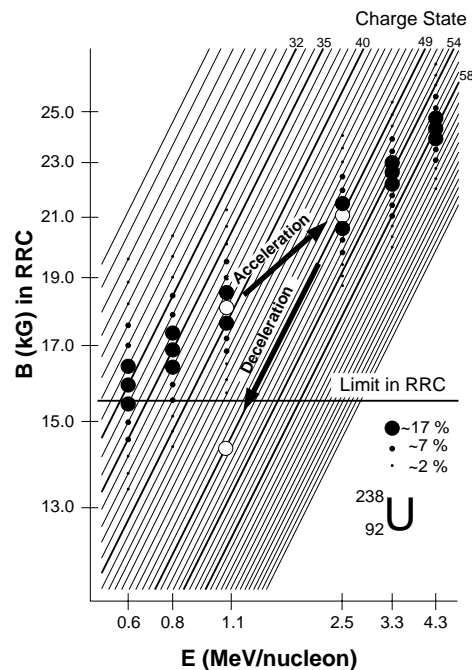


Fig. 3 Principle of the CSM: Size of a dot corresponds to the yields of U ions with re-spective charge states at the stripping (a carbon foil) energy, E. The ordinate represents the necessary bending power in the RRC.

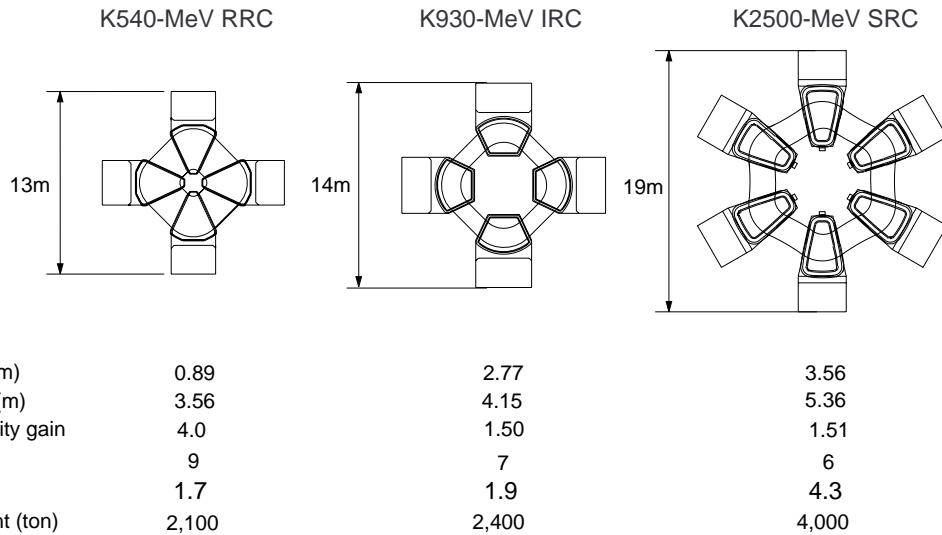


Fig. 4 Comparison of three ring cyclotrons.

the SRC can also be made to be similar to those of the RRC. Therefore, our effort has been concentrated mainly on the design of the SRC, in particular, on that of its superconducting sector magnets [5] and superconducting injection and extraction systems [6].

As shown in Fig. 5 the IRC's maximum energies are 127 MeV/nucleon for light ions up to around Ar, 102 MeV/nucleon for  $\text{Kr}^{30+}$ , and 58 MeV/nucleon for  $\text{U}^{58+}$ . The minimum energy is 25 MeV/nucleon. In the SRC the maximum energies are increased to 400 MeV/nucleon for light ions up to around Ar, to 300 MeV/nucleon for  $\text{Kr}^{30+}$ , to 150 MeV/nucleon for  $\text{U}^{58+}$  and to 100 MeV/nucleon for  $\text{U}^{49+}$ . The minimum energy is 60 MeV/nucleon.

We have undertaken the fabrication of a full-scale model sector magnet of the SRC without a yoke to verify

the mechanical and cryogenic design [7]. The superconductors for the main and trim coils have already been complete. This task is scheduled to be finished by the spring of 1998.

In this two-stage cyclotron scheme the simultaneous utilization of the HI beams is possible in both of the existing experimental facility and the new facility, when part of the IRC beam is charge-stripped and is transferred back to the existing facility. As an example, part of a 127 MeV/nucleon  $^{16}\text{O}^{7+}$  beam from the IRC, the main part of which is injected to the SRC, is charge-stripped to  $\text{O}^{8+}$  and delivered to the existing facility where the magnetic rigidity of this  $\text{O}^{8+}$  beam can be accepted.

### 3 MULTI-USE EXPERIMENTAL STORAGE RINGS (MUSES)

The MUSES (Multi-USE Experimental Storage rings) consists of an Accumulator-Cooler Ring (ACR), a Booster Synchrotron Ring (BSR) with an injector electron linac and Double Storage Rings (DSR). It will be installed downstream from the SRC and an RI beam separator, Big-RIPS.

The ACR functions for accumulation and cooling of RI (HI) beams, and is also used for atomic and molecular physics experiments with a cooler electron beam. The BSR works solely for the acceleration of RI (HI) and electron beams. The DSR permits various types of unique colliding experiments: RI (HI) - HI

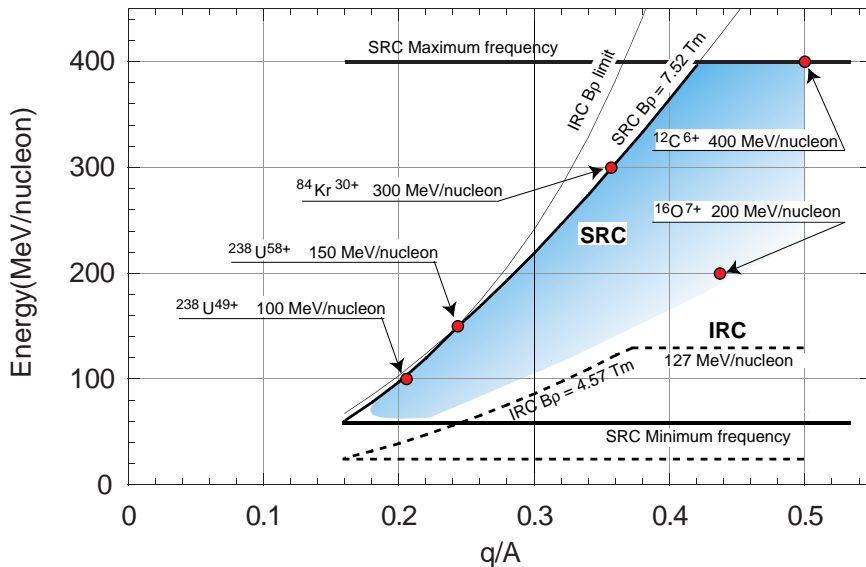


Fig. 5 Maximum HI-beam energy obtainable by the IRC and the SRC for ion species with different charge-to-mass ratios,  $q/A$ .

merging or head-on collisions; collisions between electron and RI (HI) beams; and collisions of RI (HI) beams with a high brilliant X-ray emitted from an undulator which is inserted in one ring of the DSR.

### 3.1 Production of RI Beams

The SRC's HI beams irradiate a production target and are converted to RI beams through the projectile fragmentation. RI beams generated are the mixture of various RI's; and therefore, they will be purified by means of momentum and charge-state selection at Big-RIPS.

Production rates of RI beams were theoretically estimated with the computer code INTENSITY2 [8]. In the code, physical nature of projectile fragmentation process is empirically treated. Kind of primary beam and thickness of the Be production target were optimized so as to obtain the maximum production rate. Figure 6 shows the result of estimation with the assumption that intensity of the primary HI beam is 1  $\mu\text{A}$ , and that the acceptance of the Big-RIPS is 10 mrad in angle and 1 % in momentum.

Typical RI-beam quality was also estimated: the momentum spread is  $\pm 0.5\%$ ; the phase width relative to RF frequency is  $\pm 5$  degrees; and the transverse emittance is  $4.5 \pi$  mm-mrad in both horizontal and vertical directions. This beam is transported from the production target point to the injection point of the ACR along the length of 70 m. At the end point of transport line, a

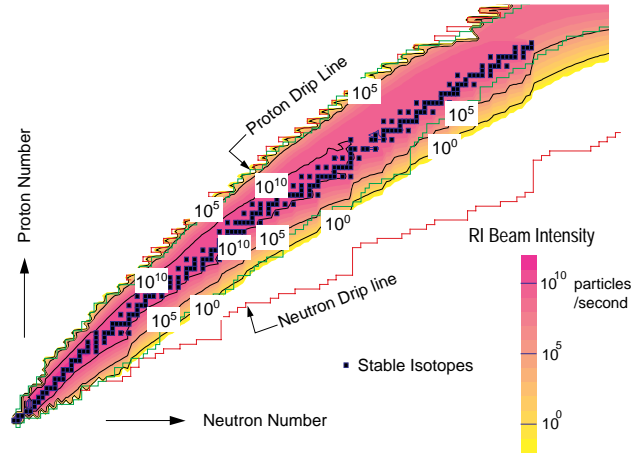


Fig. 6 Production rate of RI-beams per 1  $\mu\text{A}$  primary beam.

debuncher system with a voltage of 8 MV and harmonics number of 6 will be installed to reduce the momentum spread to  $\pm 0.1\%$ .

### 3.2 Accumulation and Cooling of RI beams in ACR

Figures 7 and 8 show the time chart for the accumulation process of RI beams in the ACR. RI-beam bunches coming from the Big-RIPS are injected into the ACR by means of the multi-turn injection. Then the rf-stacking associated with the beam cooling is performed. Momentum cooling continuously works during the rf-stacking. This process is repeated at intervals of the rf-stacking time of 30 ms plus the cooling time  $\tau_{cool}$  depending on the RI-beam property.

Simulation study for both of the electron cooling and the stochastic cooling of RI beams was done [9]. As a result, it turned out that the stochastic cooling is much faster than the electron cooling. An electron cooler with length of 3 m and current density of  $0.5 \text{ A/cm}^2$  gives, for example, the cooling time of 380 s for  ${}^6\text{He}$  and 0.42 s for  ${}^{232}\text{U}$ , whereas a stochastic cooling system composed of a 10 kW feed-back amplifier with a band width of 2 GHz gives 0.20 s and 5.0 ms, respectively. This is due to the property of the RI beam: the intensity is rather weak; and both of the momentum and emittance spreads are large.

The RI beam accumulated in the ACR decays with its own intrinsic life time  $\tau_{life}$ . The number  $N_{total}$  of the RI ions stored in the ACR after the period of  $\tau_{life}$  is determined by the balance of the supply rate and the decay rate as shown in Fig. 8. The space charge limit was also considered in the estimation of the maximum number of RI ions stored in the ACR. This limit, however, becomes effective only for RI ions neighboring on the stability line with high production rate.

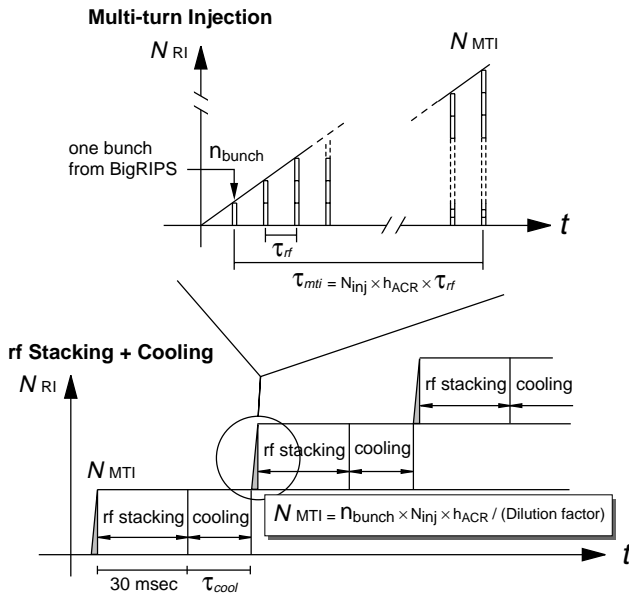


Fig. 7 Time chart of multi-turn injection (top) and rf-stacking plus cooling (bottom) in the ACR. In the figure  $n_{bunch}$  denotes the number of RI ions in one bunch coming from the Big-RIPS per  $\tau_{rf}$  ( $=1/38\text{MHz}-1/18\text{MHz}$ ),  $N_{inj}$  the number of injected turns ( $\sim 40$ ), and  $h_{ACR}$  harmonics of the ACR ( $=30$ ).

The accumulated RI beams in the ACR will be fast extracted and one-turn injected into the BSR (see Fig. 8.)

### 3.3 BSR

In the BSR, RI (HI) beams will be accelerated to the energy required for the experiment within 0.3 s, and then will be one-turn injected into the one ring of the DSR (see Fig. 8.) The maximum energies are: e.g., 1 GeV/nucleon for  $^{238}\text{U}^{92+}$ , 1.5 GeV/nucleon for ions of charge-to-mass ratio ( $q/A$ ) of 1/2 and 3.5 GeV for protons [10]. The slow-extraction channel will also be prepared.

Electrons are accelerated up to 300 MeV by an electron linac and then injected to the BSR. The BSR boosts the electron energy up to 2.5 GeV at the maximum and supply them to the one ring of the DSR. The expected beam current in the DSR is about 500 mA. In order to make a synchronous collision of electrons and RI (HI) ions, the bunch number of electrons are varied from 30 to 45 according to the ion beam energy from 300 MeV/nucleon to 3.5 GeV/nucleon. The numbers of electrons in a bunch are then  $9 \times 10^{10}$  and  $6 \times 10^{10}$ , respectively.

### 3.4 DSR

The DSR consists of vertically-stacked two rings of the similar specification. Each lattice structure takes the form of a racetrack to accommodate two long straight sections. These straight sections of one ring vertically intersect those of the other ring at two colliding points: one point is used for the collision between an RI beam and an electron beam at a collision angle of 20 mrad and the other for the merging of RI (HI) beams at a merging angle of 170 mrad. RF cavities and beam injection devices are placed at these long straight sections. Two short straight sections will be used for electron coolers to suppress the beam instabilities and to make a short-bunch ion beams [11].

The ring circumference is 269.6 m, which is 48/6 times the extraction circumference of the SRC, 33.7 m. It means that the harmonic number of the DSR is 48 while that of the SRC is 6. The maximum  $B\rho$ -value becomes 14.6 Tm when a dipole field strength is 1.5 T at the maximum. Accordingly the maximum energy is 1.0 GeV/nucleon for  $\text{U}^{92+}$  ions, 1.5 GeV/nucleon for light ions of  $q/A=1/2$ , and 3.5 GeV for protons [12].

One of typical experiments conducted at the DSR is the collision of an RI beam with an electron beam to precisely measure charge-density distribution of unstable nuclei [13]. In the experiment, one ring of the DSR will be filled with a high-current electron beam of nearly 500 mA with the energy of up to 2.5 GeV. The lattice of this electron ring is designed so that the emittance of electron beam is  $10^{-6} \pi$  m-rad from the point of view of the luminosity and beam-beam effect. The parameters of the ion ring are different from those of the electron ring because of the difference between lattices of the colliding

section in two rings. Another usage of an electron beam is to generate high brilliant X-ray by an undulator inserted in the electron ring [14]. This X-ray will shine Li-like RI ions circulating in the other ring. By detecting fluorescence emission from the ions, new spectroscopy of unstable nuclei will be possible. For this purpose the electron-beam emittance is required to be as small as  $10^{-8} \pi$  m-rad. This is achieved by forming the Double Bend Achromat (DBA) system in the arc.

## 4 CONSTRUCTION SCHEDULE

In the present schedule, the IRC, the SRC, the Big-RIPS and the experimental installation will be completed in 2002. The construction of the MUSES is planned to start in 2003 and to be fully finished in 2009.

## REFERENCES

- [1] T. Kubo et al., Nucl. Instrum. Meth., **B70** (1992) 309.
- [2] O. Kamigaito et al.: in this proceedings.
- [3] T. Nakagawa et al.: in this proceedings.
- [4] T. Mitsumoto et al.: in this proceedings.
- [5] T. Kawaguchi et al.: in this proceedings.
- [6] J.-W. Kim et al.: in this proceedings.
- [7] S. Fujishima et al.: in this proceedings.
- [8] H. Okuno et al.: in this proceedings.
- [9] T. Tominaka et al.: in this proceedings.
- [10] T. Kubo et al.: in this proceedings.
- [11] J. A. Winger et al.: Nucl. Instrum. Meth., **B70** (1992) 380.
- [12] Y.J. Yuan et al.: Proc. of EPAC96 (1996) 1338.
- [13] T. Ohkawa et al.: in this proceedings.
- [14] M. Takanaka et al.: in this proceedings.
- [15] N. Inabe et al.: in this proceedings.
- [16] T. Katayama et al.: Proc. of 3rd Intl. Conf. on Nuclear Physics at Storage Rings, Bernkastel, Germany (1996), to be published in Nucl. Phys. A.
- [17] M. Wakasugi et al.: in this proceedings.

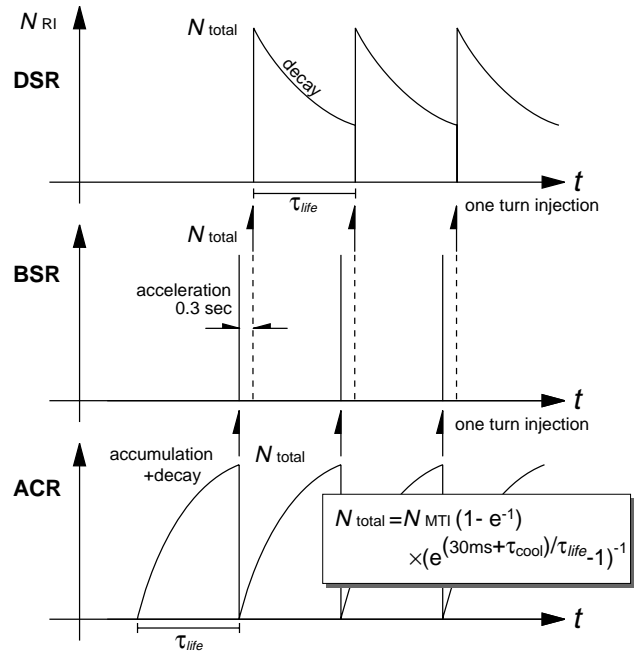


Fig. 8 Time chart of accumulation and acceleration of RI ions in the ACR, BSR and DSR.